Polar edges and their consequences for the structure and shape of hBN islands

Bene Poelsema, Adil Acun, Lisette Schouten, Floor Derkink, Martina Tsvetanova, Zhiguo Zhang, Harold J.W. Zandvliet, Arie van Houselt

Physics of Interfaces and Nanomaterials, MESA+ Institute for Nanotechnology, University of Twente, P.O.B. 217, 7500AE Enschede, The Netherlands

Abstract

The ionic component of the strong bond in hexagonal boron nitride (hBN) has been grossly disregarded in literature. Precisely this quantity is demonstrated to govern the shape of monolayer hBN islands grown at high temperatures. HBN zigzag edges are charged and energetically less favorable than the neutral armchair edges, in contrast to those of the purely covalent graphene. Nucleation of hBN islands occurs exclusively on either the inner or the outer corners of substrate steps. Taking into account the charge at edges of hBN islands offers a powerful framework to understand the nucleation of the islands and their orientation with respect the founding steps, as well as various equilibrium shapes, including prominently a right-angled trapezoid. BN dimers are identified as basic building blocks for hBN. A surprisingly strong interaction between hBN and the pre-existing steps on the moderately reactive Ir(1 1 1) substrate is uncovered. Localized charges are probably relevant for all 2D-materials lacking inversion symmetry.

Keywords: hexagonal boron nitride, nucleation and growth, sp^2 hybridization, charged edges, equilibrium shapes, Schmoluchowski effect, Low Energy Electron Microscopy

The discovery of the spectacular properties of graphene has revolutionized the interest in two-dimensional (2D) materials[1,2]. This holds in particular for the other group IV allotropes silicene and germanene[3,4,5,6] and, on the same tide, transition metal dichalcogenides (TMDs) as MoS_2[7,8]. For applications such as electronic, magnetic and (chemical) sensor devices, it is crucially important that these 2D materials can be decoupled from metallic substrates and from each other[9,10,11,12]. Insulating hexagonal boron nitride (hBN) films[13] are widely believed to provide a viable solution and are frequently referred to as "white graphene". HBN grows in a self-limited fashion as a III-V insulating monomolecular, sp^2-hybridized layer on many metal substrates, with a bandgap of about 6 eV[14,15]. Ir(111) is a preferred substrate due to the suitable lattice match and a moderately weak binding. The hBN monolayers form moiré structures with a strong tendency to align with the substrate[14,16,17,18,19,20]. In general the structural characteristics of hBN and graphene on Ir(111) show distinct similarities[21,22,23,24,25,26,27,28,29].

In the euphoria evolved on the promising potential of combining graphene with hBN for innovative applications, the decisive role of the ionic components of the boron-nitrogen bond in the growth of ultrathin hBN layers has passed grossly unnoticed. It leads to polar edges which give rise to a divergent Coulomb contribution to the total edge energy (see Supplementary information section I). Our Low Energy Electron Microscopy (LEEM) data reveals a direct relation between polar binding and the shape of hBN monolayers and provides insight in the nature of the growth precursor. Surprisingly, a strong *mutual* interaction between the "Van der Waals" film and the substrate plays an additional role in the shape of hBN monolayer islands.

In their seminal contribution on hBN on Ir(111), Farwick zum Hagen *et al*[14] reported a coincident moiré unit mesh of (12x12) hBN cells on (11x11) Ir substrate cells with two oppositely oriented phases. The moiré unit cell is mainly flat with the BN rings about

3.58 Å above the uppermost Ir(111) layer. The moiré unit cell contains a distinct valley with a minimum height of BN of about 2.07 Å above Ir(111), which anchors the moiré pattern to the substrate[14].

Figure 1 shows snapshots from a LEEM movie taken during growth of hBN on Ir(111) at 1150 K (see Supplementary Information section II). The darkish lines show monoatomic steps, multiple steps or step bunches on clean Ir(111). The dark areas represent growing hBN islands. In all our experiments they nucleate exclusively at steps and initially they have an isosceles (almost equilateral) triangular shape. This threefold symmetry reveals that the island edges preferentially orient along a specific high symmetry direction of the 2D hBN film. Two oppositely oriented isosceles triangles are distinguished. Oppositely oriented triangular islands may start their evolution from the same step. This implies that nucleation can occur at the inner (lower) side of the step as well as at the outer (upper) side of the step. From the about equal occurrence of the events we conclude that there is little to no energetic difference for both types of islands. This is further corroborated by their similar growth rates.

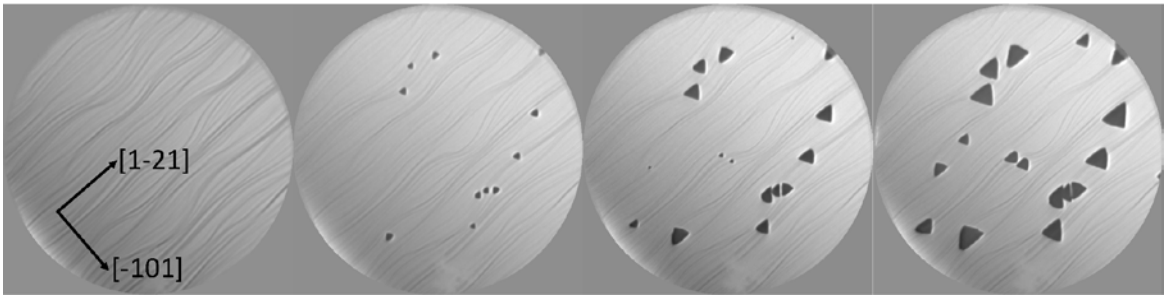

Figure 1: Growth of triangular hBN islands.
Snapshots from a LEEM movie taken during growth of hBN (black features) at 1150 K. Field of view is 20 µm, electron energy 17 eV. Curved lines represent steps which are globally oriented along the [1-21] direction.

The internal structure of hBN in the oppositely oriented triangles is oppositely oriented as well. Figure 2 shows two selected area diffraction (µLEED) patterns, obtained with an aperture size of 1.4 µm. The patterns are characteristic of oppositely oriented triangles.

The data, taken at 35 eV, shows that the moiré pattern as revealed by the fine structure in the diffraction pattern is nicely aligned to the substrate. The overall patterns are threefold symmetric in both cases, due to the FCC structure of the Ir(111) substrate. The threefold symmetry is rotated by 180^{o} for the two patterns. This implies that the opposite orientation of the triangles is accompanied by a 180^{o} rotated atomic arrangement inside the triangular hBN islands.

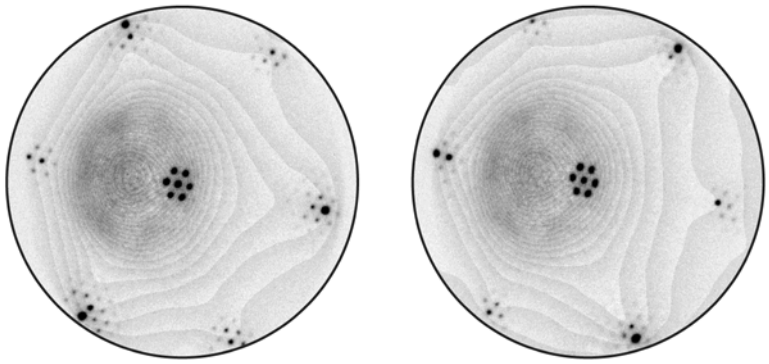

Figure 2: Orientation of the oppositely oriented triangles
Contrast inversed (bright to dark spots) µLEED patterns from representatives of both island types. Aperture 1.4 µm and electron energy 35 eV. The darkish area left from the specular beam is due to secondary electrons, including inelastically scattered ones. The curved lines are an artifact due to digital noise.

The simultaneous presence of both orientations is in line with the vast majority of the literature on the hBN/Ir(111) system, following the pioneering paper by Auwärter *et al.*[30], where this observation was first made for hBN on Ni(111) using a photo-electron diffraction technique. These observations are explained by a preference for the boron atoms to occupy threefold hollow sites on Ir(111), while the N atoms prefer on top positions. For one type of flakes the B atoms occupy preferably HCP sites (above a *second* layer Ir atom) and take FCC positions (above a *third* layer Ir atom) for the other one. The site description holds for the B and N atoms in (and next to) the valleys, where they are strongly bound. We refer to these types as H-hBN and F-hBN, respectively.

The threefold symmetric shape of the islands indicates that their edges are of either the zigzag- or the armchair type[31] (See also Supplementary information section III for a sketch and an estimation for the difference in edge energies).These are oriented along the <1-10> and the <-1-12> azimuth directions of the Ir(111) substrate, respectively.

For reasons that become evident below we consider the armchair (along <-1-12>) as the favored edge. This situation is sketched in Fig. 3 for a commensurate hBN structure, while in reality the hBN is only higher order commensurate with (12x12) hBN unit cells residing on (11x11) Ir(111) unit cells. In the valleys of the moiré pattern the B and N atoms are chemically

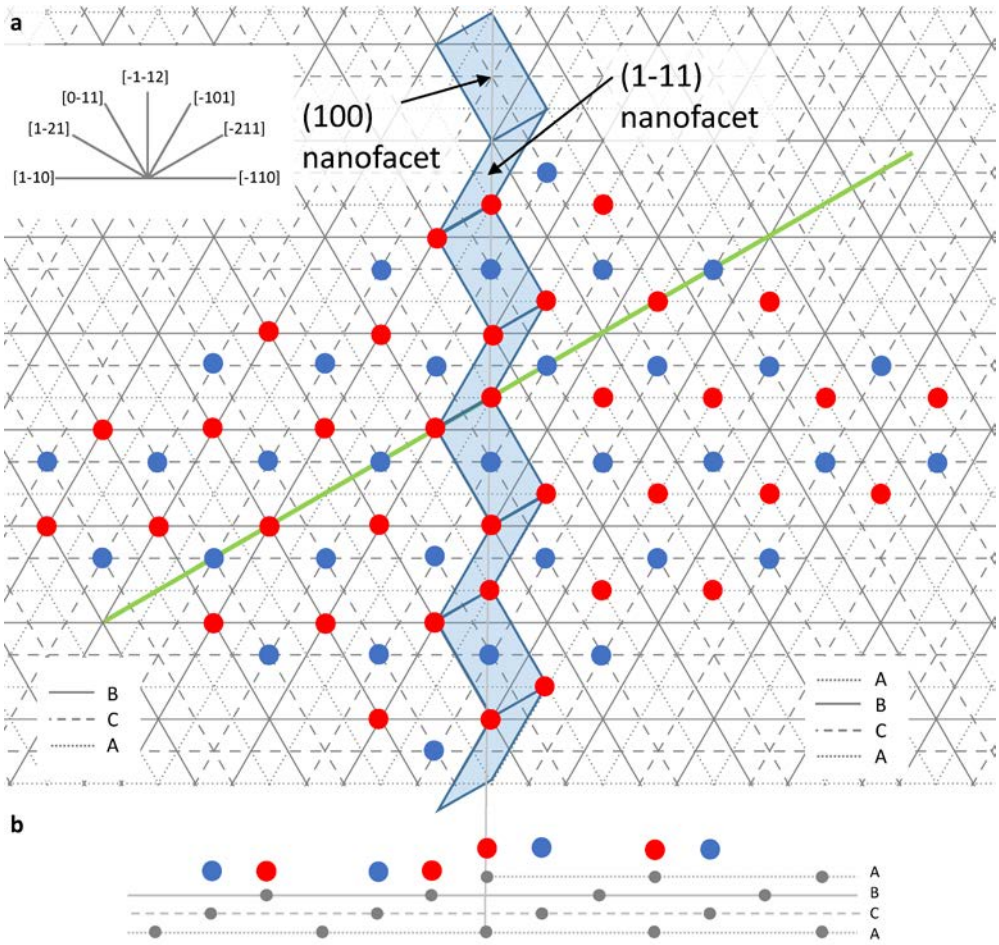

Figure 3: Schematic representation of triangular hBN islands.
a. Top view of the Ir(111) substrate with the atomic layer levels indicated by A, B, and C (see inserts). A [-1-12] oriented atomic step is sketched in the center (azimuth directions are indicated in the upper left insert). The step up direction is from left (stacking order BCABCA) to right (stacking order ABCABC). The (1-11) and (100) nanofacets within the step are indicated by the blue rhombi and rectangles, respectively. Triangular sp^2 hybridized hBN islands are shown on the different terraces, with the B- and N-atoms as blue and red circles, respectively. **b.** Side view along the [-211] direction (left to right).

bound to the substrate. The B and N atoms outside the valleys assume less well-defined positions with respect to the Ir(111) unit cells and are much more weakly bound to Ir[14].

Fig. 3 sketches the situation in the valleys of the moiré profile with strong binding (chemisorption). The left and right hand side triangles represent H-hBN and F-hBN, respectively. Note that the size of the valleys is much smaller than the area shown in Fig. 3.

The distinct role of the steps is already clear from the observation that nucleation of hBN islands occurs exclusively on step edges. This holds strictly for the relatively high growth temperatures in the present study. The nucleation occurs at about equal rates on top of steps as well as at the inner corners. These nucleation sites appear to pin the moiré plates and consequently determine whether the hBN islands are of H- or F-type. This specific nucleation behavior is attributed to the consequences of Smoluchowski smoothing of the electron density contour around atomic steps[32]. This leads to the formation of dipoles around steps with a reduced electron density at the upper part of the step and excess electron density at the inner corners. As a result, the work function of metal surfaces decreases with increasing step density[33]. Electron density smoothing at steps has been demonstrated directly by thermal helium atom scattering, which senses electron density contours[34]. The Smoluchowski effect at steps is generic and is increasingly significant for more open step directions, i.e. it is stronger for <-1-12> steps than for <1-10> steps. It may even result in sizeable inward relaxation of the protruding upper step atoms[35]. The decisive role of the steps for the growth of H- or F-type hBN is now understood straightforwardly. An N atom (red) carries a net negative charge and a B atom inside hBN is positively charged[36]. Consequently, the N atom at the hBN edges is bound most strongly on top of the protruding Ir atom in the upper level with lacking conduction electrons. From there the B and other N atoms assume sites governed by the threefold symmetries of Ir(111) and hBN. As illustrated in Fig. 3, this gives rise to the growth of F-type hBN when nucleation takes place at the upper step edge. In a similar way when nucleation takes place at the lower step edge, the B atom (blue) with net positive charge, takes a position with the highest coordination and excess electron density, which is (close to) the centre of the (1-11) nanofacets inside the step. From there the hBN grows naturally as H-type following the rules imposed by the threefold

symmetry of both hBN and Ir(111). This way we find a natural explanation for the anchor sites of the moiré pattern, the type of the resulting hBN and the direction of growth observed experimentally. An attendant argument for the resulting orientation of the flakes is that all edges are of the armchair type. Within one period along the edge the outermost B and N atom lack both one binding partner compared to atoms in the interior of the hBN island. As a result they will be charged. Their net charges, however, cancel each other and the total (straight) edge is therefore charge neutral.

The morphology and detailed growth behavior of both types of triangles differ during more advanced stages of growth. In order to understand the different propagation of hBN across substrate steps we consider its moiré structure in some more detail. It consists of dominant “flat” Van der Waals parts at a distance of about 3.58 Å above the outermost Ir(111) layer. It has relatively deep and narrow valleys in which the B and N atoms are chemically bound and locally reside at only about 2.07 Å above Ir. These valleys function as anchor sites and determine the alignment with respect to the Ir(111) and also whether one deals with H-hBN of F-hBN locally. The distance between two adjacent valleys is about 42 Å along the close packed directions on Ir(111). Nucleation of hBN takes place on either the outer or the inner corner of a [-1-12] oriented step, which leads to oppositely oriented isosceles triangles; several examples are displayed in Fig. 1. The occurrence of both types is about equal, which applies also for their growth rates. However, the motion of their centre of gravity is different. This is illustrated in Fig. 4. The sketch in 4a shows a triangular island of which the horizontal side is pinned at the lower side of an atomic step and the island grows from high to low. The sketch in 4b shows also a triangular island. It nucleated at an atomic step, but this time it is able to grow across a descending step. This behavior agrees with the actually measured situation underneath. A possible minor thermal drift would be identical in both cases. For islands nucleated at the outer corners (right hand side) the first anchoring sites are close to the descending step and the moiré surface can simply expand from the step. The Van der Waals part of the profile can easily bend and nestle to the lower terrace before a next valley is formed at a lateral distance of ~42 Å. After nucleation in the inner

corner near an ascending step the islands also grows readily away from the corner. However, crossing the ascending corner is now much more difficult since the Van der Waals part of the profile must be lifted by an additional 2.22 Å being the Ir(111) step height along a small lateral distance of a few Ångstroms. The required bending is quite severe and is considered unlikely. This reasoning implies that the staircase formed by the step trains in Fig. 4 (and in Fig.1) goes downward in the direction of the arrow (from upper left to lower right).

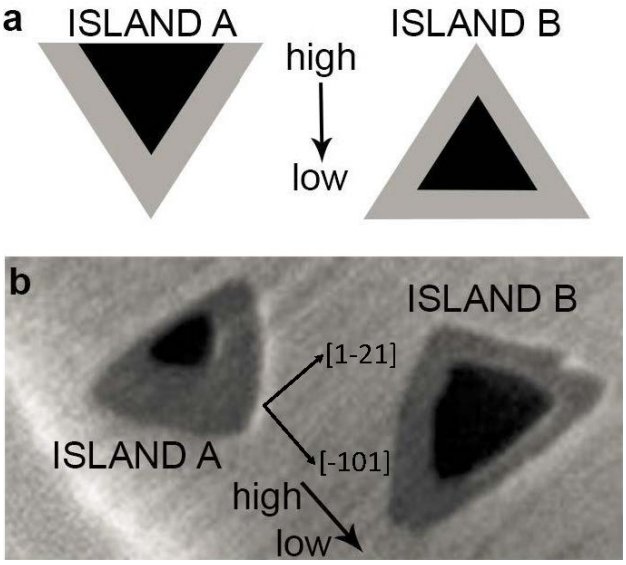

Figure 4: Growth of triangular islands across terraces
HBN islands at early (black) and a more advanced stage of growth (grey). **a.** Idealized sketch of triangular hBN islands nucleated at an atomic step. **b.** Corresponding experimental islands taken from a movie during growth. The greyish lines represent pre-existing steps on Ir(111). Field of view 3.2 x 5.8 μm^2. The azimuth directions are indicated.

Figure 5a shows a LEEM image of a clean Ir(111) sample taken at 1150 K. This picture is, at first sight, a great surprise. Two distinct areas, area I (bottom) and area II (top), are observed on which the slightly curved features, which are attributed to step(bunche)s, as in Fig. 1, are oriented perpendicular to each other. The line separating both areas is strikingly straight. We have carefully looked into the possibility of mozaic structures (microcrystallites) to explain this observation. To this end we compared µLEED patterns taken at areas I and II at a broad range of electron energies from about 40 to 200 eV. No differences between both sets are observed (cf Figs. 5b and 5c). This way we rule out

199 the possibility of different local crystal structures to explain the difference between
200 areas I and II. As the only possible result one is left with the predominance of steps in
201 both areas along 90° different azimuth directions. It is well known that for pristine metal
202 fcc (111) surfaces the atomic steps are preferentially oriented along <1-10> directions.
203 We call these the areas I. The areas II then represent those with dominant <-1-12>
204 steps. We note that these step features cannot cross and therefore a straight line

205

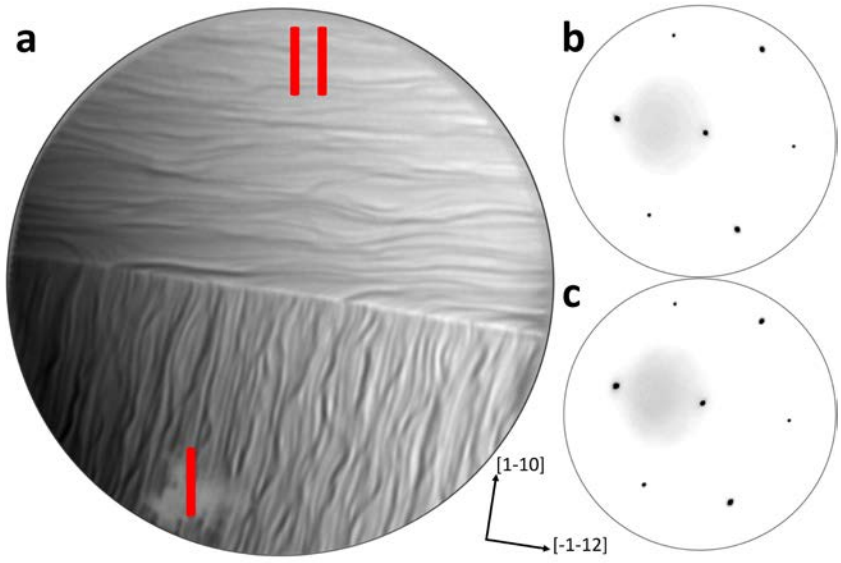

Figure 5: Different preferred step directions after hBN growth
a. LEEM image of clean Ir(111), FoV = 25 µm, electron energy 2.5 eV. µLEED patterns measured with 41.5 eV electron energy for the upper (**b**) and lower (**c**) part of the image in **a**. The substrate temperature was about 1150 K. The indicated crystallographic directions apply to all panels.

206

separating both areas fits in this picture. Energetically both step orientations should be quite similar. Steps up and steps down along <1-10> have either {111} or {100} nanofacets, which are very similar in energy[37,38,39]. The steps along <-1-12> also have {111} and {010} nanofacets (cf. Fig. 3). A strong interaction between hBN and the steps is held responsible for the observed evolution of the preferred step direction. If that interaction favors the evolution towards <-1-12> oriented steps an increasing integral area II should evolve at the cost of the integral area I. Prolonged hBN growth

experiments at relatively high temperatures (900 – 1200 K) then favor a general rotation of the preferred step orientation away from <1-10> towards <-1-12>. In all cases, both areas would remain well separated due to forbidden step crossings. This is exactly what happens after prolonged hBN growth study at high temperatures. We have found an increasing preference for areas II in the course of our prolonged hBN/Ir(111) growth study (See supplementary information section IV for a discussion on the temporal evolution of the change from areas I to II).

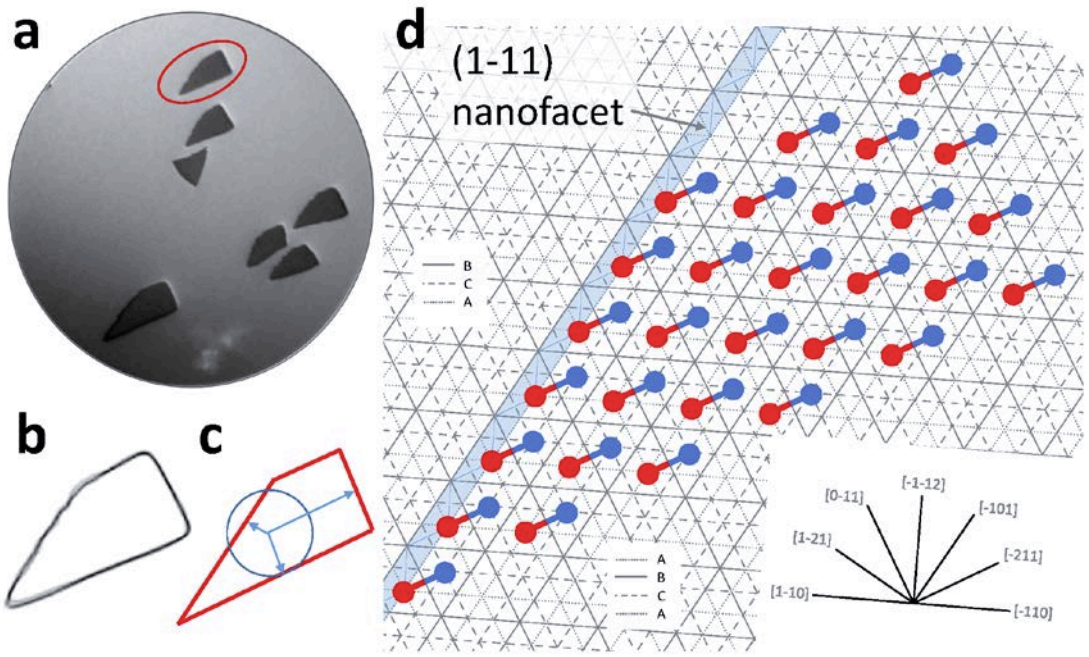

Figure 6: Growth of trapezoidal and triangular hBN islands.
a. Snapshot from a LEEM movie (field of view is 20 µm, electron energy 16.3 eV) during growth of hBN on a fresh Ir(111) sample at 1200 K. **b.** Normalized contours of 350 subsequent images of the right-angled trapezoidal hBN islands highlighted by the red ellipse in a) The sharp lower left angle is 30°. The left edge nucleated at the [-101] step of the Ir(111) surface. The areas vary between 0.9 and 4.1 µm^2. **c.** Sketch of the corresponding Wulff plot (red lines). **d.** Schematic representation of the right-angled trapezium highlighted by the red ellipse in **a**. The island is of H-hBN type. The (1-11) nanofacet is indicated by the blue stripe. A similar sketch is possible for {100} nanofacets. The constituting B (blue) – N (red) dimers are indicated.

The local preference for steps along <1-10> (area I) or along <-1-12> (area II) leads to pronounced differences in the relative abundance of type H- or type F-hBN. Figure 1 shows snapshots taken from a LEEM movie during the growth of hBN on an area of type II. Figure 6a shows a characteristic snapshot of a LEEM movie (see Supplementary Information section V) taken during initial hBN growth on a fresh Ir(111) substrate. The predominant step orientation is therefore along <1-10> directions[37] and the host area is of type I. In contrast to the situation in Fig. 1, triangular islands form a distinct minority. The most abundant hBN islands, nucleated on the [-101] steps in Fig 6a, do not have a triangular shape, but rather exhibit a trapezoidal shape. During the initial stages of the growth, where the mutual influence on and by neighboring islands is still small, these islands have a right-angled trapezoidal shape (see Fig 6a). In the extreme case, they are characterized by sides which make angles of 30° and 90° with the longest one of the two parallel sides. This particular shape is unveiled as the equilibrium shape for islands nucleated at straight [-101] step segments with (1-11) nanofacets. This is confirmed by the data gathered in Fig. 6b for a large number (350) of successive images of the right-angled trapezoidal hBN island highlighted by the red ellipse in Fig. 6a. Fig. 6b shows the normalized outer contours of the island for varying areas from about 0.9 to about 4.1 μm^2. Indeed the shape is identical and does not depend on the size of island. A similar analysis for islands nucleated at different <-101> steps leads to identical results. Minor differences on the left- and right-hand edges are expected and observed due to the strong inherent dependence on the *local* shape of the founding <-101> steps. We note that considerable deviations from the equilibrium shape occur for larger islands. Depending on whether mass transport occurs via edge diffusion or via 2D surface diffusion the involved times required for establishing equilibration shapes scale with a power law, i.e. as A^4 or A^2, for an island of size A, respectively[40]. The time constant in the experiment is fixed and given by the rate of incidence of the borazine molecules, their decomposition rate and the incorporation rate of the borazine fragments (BN-dimers). Consequently, beyond a given size the islands can no longer maintain their equilibrium shape during progressing growth stages. Departure from equilibrium will also occur

through direct or indirect interactions (shadowing) with neighboring islands. Therefore, the discussion below focuses on initial stages of growth.

The equilibrium shape of hBN islands nucleated at pre-existing [10-1] on type I regions of Ir(111) is now completely defined. The edge of the islands at the parent step is of the zigzag type. The edges pointing away from the ascending step make an angle of 30° with the step and align along the [-211] azimuth and are thus of the armchair type. The remaining edge exhibits a right angle to [-211], i.e. is aligned along [0-11] (see Fig. 6d). Note that this edge is not of zigzag type, but rather boron terminated. This experimental fact allows important conclusions on the elementary building blocks for the hBN islands. With increasing temperature first dehydrogenation of the borazine molecules takes place. On most metals, in particular transition state metals, the resulting H-atoms desorb associatively. The other extreme at very high temperatures is a complete decomposition as the borazine molecules fall apart in B and N atoms. In that case the nitrogen atoms also desorb associatively, leaving B behind. Such is indeed the case for hBN at higher temperatures than currently considered situation[21]. This situation impairs the balance between N and B atoms required to grow hBN and must be avoided. As a result hBN grows from well defined fragments as either dehydrogenated $(BN)_3$ rings or BN dimers. The latter is particularly stable due to the combination of covalent bonding and ionic bonding. It is impossible to arrive at a hBN-island with the obtained equilibrium shape by successive incorporation of intact $(BN)_3$ rings. The successive addition of aligned BN dimers is the only option to grow the observed equilibrium shape, as illustrated in Fig. 6b. We therefore conclude that BN-dimers constitute the basic building blocks for the growth of hBN on Ir(111) at 1200 K.

The zigzag edge at the parent [-101] step is charged as the terminating N atoms lack each one B nearest neighbor when compared to an N atom in the centre of the island. The built-in charge along the [-101] step is compensated at the opposite [0-11] edge, which is a natural consequence when the hBN islands are built from BN dimers. The terminating [0-11] edge consists of BN dimers of which each B atom lacks two N nearest

neighbors. The positive charge density of the [0-11] edge is therefore twice as high as that of the negative [-101] edge along the Ir [-101] step and charge neutrality is maintained. We emphasize that the armchair edges [-1-12] and [1-21] are missing in the shape of the right-angled trapezium. A close inspection of Fig. 6d reveals that these edges cannot be constructed from BN dimers after nucleation of the island at the [-101] step. Therefore, these missing "inexpensive" edges provide additional evidence that BN-dimers act as the basic building blocks of the hBN island. Figure 6c shows a sketch of the Wulff plot for the equilibrium shaped island in Fig. 6b. The lowest edge energy is along the founding [-101] step, a relatively low edge energy is realized along [-211], while an energetically unfavourable B termination is achieved along [0-11] by a row of BN dimers.

The right angled trapezium shape establishes an extreme. For a slightly curved parent step the edge of the hBN island is composed of a combination of zigzag and armchair segments. Therefore, the opposite edge of the island must be composed of corresponding segments in order to warrant charge neutrality. Consequently, local curvature of the parent steps has a direct impact on the island's shape. As mentioned further above the charge neutral armchair edges are energetically preferred. The fact that the island side away from the parent step is not terminated by "cheap" armchair elements is indicative of the enormous influence of Coulomb induced shape effects.

As noted earlier triangular hBN islands are only occasionally observed during growth in type I areas too. These islands also nucleate at a parent [-101] atomic step. Notably this step forms a bisector of the growing isosceles triangle (see Fig. 6a for an illustration). The edges of the isosceles island are again along <11-2> Ir azimuths and are thus of the favorable, energetically cheap, armchair type. The hBN structure inside the triangular islands is rotated by 180° (or 30° ± n·120°) compared to the predominant trapezoids. Attempts to construct isosceles triangular F-hBN islands with a bisector along a <-101> and armchair edges, however, fail. They all lead to a non-negligible charging at the bisector. It builds up linearly with the growing island size. We suggest that nature does better and propose a model for the triangular islands, shown in Fig. 7. The parent [-101]

step forming the bisector, is indicated with blue rectangles and has (1-11) nanofacets. The first BN-dimer row is oriented perpendicular to the step. As such they are the complement of the situation of the right-angled trapezium (see Fig. 6d) where the BN-dimers in the first row are oriented at 30° from the step. All edges are of the armchair type and the total triangular island is built up from BN dimers as building blocks. It is

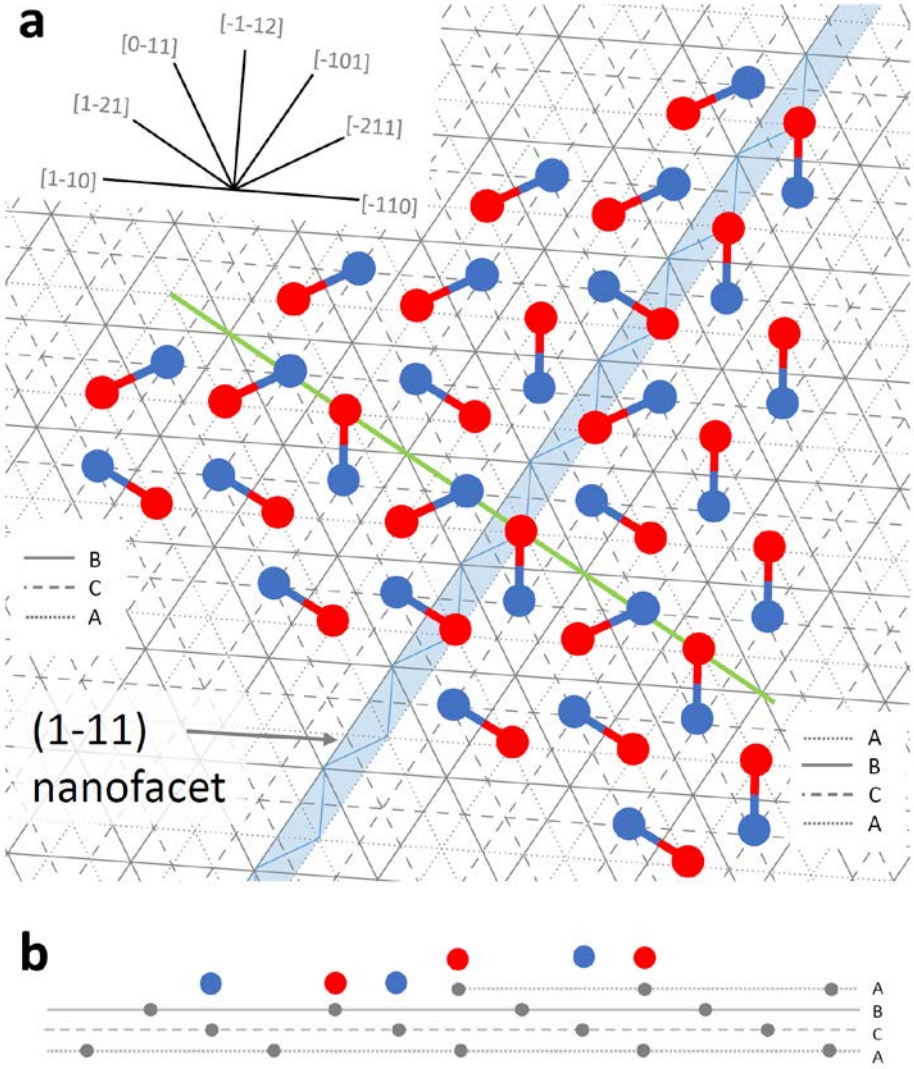

Figure 7: Schematic representation of triangular hBN islands with <110> steps as bisector

a. Schematic representation of the triangular hBN islands in Fig 4a. The [-101] step edge with a (1-11) nanofacet is shown by the blue rectangles. A similar sketch is possible for {010} nanofacets. The edges are of the armchair type. Step up from left to right. Left: H-hBN, right: F-hBN. The constituting B(blue)–N(red) dimers are indicated. **b.** Side view along the [1-21] direction (green line in **a**).

299 easily seen that the total construction is charge neutral and thus no Coulomb based
300 contribution to the total energy of the island is present, including the region around the
301 bisector. Further growth will maintain the energetically favored armchair edges. The left
302 half of the triangle (on the lower terrace) is of H-hBN type, while the right half (on the
303 higher terrace) is of F-hBN type. Indications for different types of hBN within one
304 triangle have indeed been observed[41]. However, we have not observed a clear
305 indication for hybrid hBN inside one island. It is easy to conceive that the structure is
306 anchored or pinned by the situation at the upper step edge (the N atoms would prefer
307 the sites on top of the step due to Smoluchowski electron density smoothening.
308 Maintaining this anchoring the hBN blanket may well be continued in the F-hBN mode.

309 Triangular hBN islands have been reported by many authors (e.g.[41,14]). Following
310 Auwärter *et al*.[30], these authors arrived at the conclusion that these triangles lead to
311 islands terminated by either B- or N-rich edges. That is correct indeed for ideal islands
312 on ideal (stepless) terraces, which require unbalanced B and N atom numbers and thus
313 total decomposition. However, our current findings show exclusive nucleation at steps.
314 Combined with BN-dimers as constituting entities, this provides a natural way to break
315 the three-fold symmetry condition and ensures balanced quantities of B and N in the
316 hBN island (edges). Our results are thus inconsistent with an exclusive B termination of
317 hBN island edges[14].

318

319 **Conclusions**

320 We demonstrate the crucial role of ionic binding aspects in hBN on the binding to
321 Ir(111), the orientations and locations of the islands and their equilibrium shapes. A
322 direct consequence of the ionic bonds is that zigzag edges are charged, while armchair
323 edges remain neutral. A careful consideration of Coulomb interactions, in combination
324 with Smoluchowski smearing of the electron density at step edges leads to a consistent
325 picture of hBN on Ir(111). Since these aspects (ionic binding and electron density
326 smearing at steps) are generic we suggest that this picture guides more generally the

understanding of hBN growth on (quite) strongly interacting metal substrates. Moreover, BN dimers are identified as the basic building blocks of the hBN islands.

Methods

An Elmitec LEEM III with a base pressure below 1 x 10^{-10} mbar was used to study the growth of hBN on Ir(111). Ir(111) single crystals (Surface Preparation Laboratory) were cleaned by subsequent alternating cycles of Argon ion sputtering and annealing in oxygen environment at 1300 K, with subsequent flash annealing at 1600 K before each measurement. HBN was removed by annealing at 1300 K and subsequently the sample was cleaned as described above. No traces of contamination were observed using Auger Electron Spectroscopy. Borazine was purchased from Chemos GmbH.

Acknowledgement

We thank the Nederlandse organisatie voor wetenschappelijk onderzoek (NWO) for financial support.

References

[1] Novoselov, K. S., Geim, A. K., Morozov, S. V., Jiang, D., Zhand, Y., Dubonos, S. V., Grigorieva, I. V. & Firsov, A. A. Electric field effect in atomically thin carbon films. *Science* **306**, 666-669 (2004).

[2] Geim, A. K. & Novoselov, K. S. The rise of graphene. *Nat. Mater.* **6**, 183-191 (2007).

[3] Vogt, P., De Padova, P., Quaresima, C., Avila, J., Frantzeskakis, E., Asensio, M. C., Resta, A., Ealet, B., & Le Lay, G. Silicene: compelling experimental evidence for graphenelike two-dimensional Silicon. *Phys. Rev. Lett.* **108**, 155501 (2012).

[4] Cahangirov, S., Topsakal, M., Aktürk, E., Sahin, H., & Ciraci, S. Two- and one-dimensional honeycomb structures of silicon and germanium. *Phys. Rev. Lett.* **102**, 236804 (2009).

[5] Bampoulis, P., Zhang, L., Safaei, A., van Gastel, R., Poelsema, B., & Zandvliet, H.J.W. Germanene termination of Ge_2Pt crystals on Ge (110). *J. Phys. Condens. Matter* **26**, 442001 (2014).

[6] Zhang, L., Bampoulis, P., Rudenko, A.N., Yao, Q., van Houselt, A., Poelsema, B. & Zandvliet, H.J.W. Structural and electronic properties of germanene on MoS_2. *Physical Review Letters* **116**, 256804 (2016).

[7] Mak, K.F., Lee, C., Hone, J., Shan, J., & Heinz, T.F. Atomically thin MoS2: a new direct-gap semiconductor. *Phys. Rev. Lett.* **105**, 136805 (2010).

[8] Li, H., Zhang, Q., Yap, C.C.R., Tay, B.K., Edwin, T.H.T., Olivier, A. & Baillargeat, D. From bulk to monolayer MoS_2: Evolution of Raman scattering. *Adv. Funct. Mater.* **22**, 1385-1390 (2012).

[9] Xu, M., Liang, T., Shi, M.& Chen, H. Graphene like two-dimensional materials. *Chem. Rev.* **113**, 3766-3798 (2013).

[10] Schulz, F., Drost, R., Hämäläinen, S. K. & Liljeroth, P. Templated self-assembly and local doping of molecules on epitaxial boron nitride. *ACS Nano* **7**, 11121−11128 (2013).

[11] Gehring, P, Gao, B.F., Burghard, M. & Kern, K. Growth of high-mobility Bi_2Te_2Se nanoplatelets on hBN sheets by van der Waals epitaxy. *Nano Lett.* **12**, 5137−5142 (2012).

[12] Dean, C.R., Young, A.F., Meric, I., Lee, C., Wang, L., Sorgenfrei, S., Watanabe, K., Taniguchi, T., Kim, P., Shepard, K. L. & Hone, J. Boron nitride substrates for high-quality graphene electronics. *Nat. Nanotechnol.* **5**, 722−726 (2010).

[13] Corso, M., Auwärter, W., Muntwiler, M., Tamai, A., Greber, T., & Osterwalder, J. Boron nitride nanomesh. *Science* **303**, 217−220 (2004).

[14] Farwick zum Hagen, F.H., Zimmermann, D.M., Silva, C.C., Schlueter, C., Atodiresei, M., Jolie, W., Martínez-Galera, A.J., Dombrowski, D., Schröder, U.A., Will, M., Lazić, P., Caciuc, V., Blügel, S., Lee, T-L., Michely, T. & Busse, C. Structure and growth of hexagonal boron nitride on Ir(111). *ACS Nano* **10**, 11012-11026 (2016).

[15] Cassabois, G., Valvin, P. & Gil, B., Hexagonal boron nitride is an indirect bandgap semiconductor. *Nature Photonics* **10**, 262-266 (2016).

[16] Dong, G., Fourré, E.B., Tabak, F.C. & Frenken, J.W.M. How boron nitride forms a regular nanomesh on Rh(111). *Phys. Rev. Lett.* **104**, 096102 (2010).

[17] Orlando, F., Lacovig, P., Omiciuolo, L., Apostol, N.G., Larciprete, R., Baraldi, A. & Lizzit, S. Epitaxial growth of a single-domain hexagonal boron nitride monolayer. *ACS Nano* **8**, 12063-12070 (2014).

[18] Orlando, F., Larciprete, R., Lacovig, P., Boscarato, I., Baraldi, A. & Lizzit, S. Epitaxial growth of hexagonal boron nitride on Ir (111). *J. Phys. Chem. C* **116**, 157−164 (2012).

[19] Usachov, D., Fedorov, A., Vilkov, O., Adamchuk, V. K., Yashina, L. V., Bondarenko, L., Saranin, A. A., Grüneis, A. & Vyalikh, D. V. Experimental and computational insight into the properties of the lattice-mismatched structures: Monolayers of h-BN and graphene on Ir(111). *Phys. Rev. B* **86**, 155151 (2012).

[20] Schulz, F., Drost, R., Hämäläinen, S.K., Demonchaux, T., Seitsonen, A. P. & Liljeroth, P. Epitaxial hexagonal boron nitride on Ir(111): A work function template. *Phys. Rev. B* **89**, 235429 (2014).

[21] Petrović, M., Hagemann, U., Horn-von Hoegen, M. & Meyer zu Heringdorf, F.-J. Microanalysis of single-layer hexagonal boron nitride islands on Ir(111). *Appl. Surf. Sci.* **420**, 504-510 (2017).

[22] van Gastel, R., N'Diaye, A. T., Wall, D., Coraux, J., Busse, C., Buckanie, N. M., Meyer-zu-Heringdorf, F., Horn von Hoegen, M., Michely, T. & Poelsema, B. Selecting a single orientation for millimeter sized graphene sheets. *Appl. Phys. Lett.* **95**, 121906 (2009).

[23] N'Diaye, A. T., van Gastel, R., Martínez-Galera, A. J., Coraux, J., Hattab, H., Wall, D., Meyer-zu-Heringdorf, F., Horn von Hoegen, M., Gómez-Rodríguez, J. M., Poelsema, B., Busse, C. & Michely, T. In situ observation of stress relaxation in graphene. *New J. of Phys.* **11**, 113056 (2009).

[24] Sutter, P., Sadowski, J. T. & Sutter, E. Graphene on Pt(111): Growth and substrate interaction. *Phys. Rev. B* **80**, 245411 (2009).

[25] Sutter, P. & Sutter, E. Microscopy of Graphene Growth, Processing, and Properties. *Adv. Funct. Mat.* **23**, 2617-2634 (2013) and references therein.

[26] Loginova, E., Bartelt, N. C., Feibelman, P. J. & McCarty, K. F. Evidence for graphene growth by C cluster attachment. *New J. Phys.* **10**, 093026 (2008).

[27] Loginova, E., Nie, S., Thürmer, K. Bartelt, N. C. & McCarty, K. F. Defects of graphene on Ir(111): Rotational domains and ridges. *Phys. Rev. B* **80**, 085430 (2009).

[28] Rogge, P. C., Thürmer, K., Foster, M. E., McCarty, K. F., Dubon, O. D. & Bartelt, N. C. Real-time observation of epitaxial graphene domain reorientation. *Nature Comm.* **6**, 6880 (2015).

[29] Rogge, P. C., Nie, S., McCarty, K. F., Bartelt, N. C. & Dubon, O. D. Orientation-dependent growth mechanisms of graphene islands on Ir(111). *Nano Lett.* **15**, 170-175 (2015).

[30] W. Auwärter, M. Muntwiler, J. Osterwalder & T. Greber, *Defect lines and two-domain structure of hexagonal boron nitride films on Ni(111)*. Surf. Sci. **545**, L735 (2003).

[31] K. Nakada, M. Fujita, G. Dresselhaus, M.S. Dresselhaus, *Edge state in graphene ribbons: Nanometer size effect and edge shape dependence*. Phys. Rev. B **54,** 17954 (1996).

[32] Smoluchowski, R. Anisotropy of the electronic work function of metals. *Phys. Rev.* **60,** 661-674 (1941).

[33] Poelsema, B., Palmer, R. L. & Comsa, G. Helium scattering and work function investigation of CO adsorption on Pt(111) and vicinal surfaces. *Surf. Sci*. **123**, 152-164 (1982).

[34] Bedrossian, B., Poelsema, B., Rosenfeld, G., Jorritsma, L. C., Lipkin, N. N. & Comsa, G. Electron density contour smoothening for epitaxial Ag islands on Ag(100). *Surf. Sci.* **334**, 1-9 (1995).

[35] Visscher, B., Boers, A. L., Verheij, L. K. & Poelsema, B. Relaxation of the edge atoms of a stepped Cu(410) surface. *Appl. Surf. Sci.* **26**, 121-128 (1986).

[36] Grad, G. B., Blaha, P., Schwarz, K., Auwärter, W. & Greber, T. Density functional theory investigation of the geometric and spintronic structure of *h*-BN/Ni(111) in view of photoemission and STM experiments. *Phys. Rev. B* **68**, 085404 (2003).
Greber, T. Graphene and Boron Nitride single layers, arxiv:0904.1520 (2009).

[37] Bott, M., Hohage, M., Michely, T & Comsa, G. Pt(111) reconstruction induced by enhanced Pt gas-phase chemical potential. *Phys. Rev. Lett.* **70**, 1489-1492 (1993).

[38] Jacobsen, J., Jacobsen, K. W. & Nørskov, J.K. Island shapes in homoepitaxial growth of Pt(111). *Surf. Sci.* **359**, 37-44 (1996).

[39] Rost, M. J., Michely, T. & Comsa, G. Comment on "Self-diffusion and dynamic behavior of atoms at step edges on iridium surfaces. *Phys. Rev. B* **57**, 1992-1994 (1998).

[40] Morgenstern, K., Rosenfeld, G., Poelsema, B. & Comsa G. Brownian motion of vacancy islands on Ag(111). *Phys. Rev. Lett.* **74**, 2058-2061 (1995).

[41] Lu, J., Yeo, P. S. E., Zheng, Y., Xu, H., Gan, C. K., Sullivan, M. B., Castro Neto, A. H. & Loh, K. P. Step flow versus mosaic film growth in hexagonal boron nitride. *J. Am. Chem. Soc.* **135**, 2368-2373 (2013).